

# **Curing, Hydration, and Microstructure of Cement Paste**

**by**

**Dale P. Bentz, Paul E. Stutzman**

**Building and Fire Research Laboratory National Institute of Standards and Technology,  
Gaithersburg, MD**

**Reprinted from ACI Materials Journal pp. 348 - 356, 2006.**

**NOTE: This paper is a contribution of the National Institute of Standards and Technology and is not subject to copyright.**

**NIST**

**National Institute of Standards and Technology**  
Technology Administration, U.S. Department of Commerce

# Curing, Hydration, and Microstructure of Cement Paste

by Dale P. Bentz and Paul E. Stutzman

*This paper compares hydration characteristics and microstructures of cement pastes with water-cement ratios (w/c) of 0.35 and 0.435, cured under saturated and sealed conditions. Degree of hydration is quantified by loss on ignition (LOI) measurements. The microstructures, and specifically the pore structures, of the hydrated pastes are evaluated using scanning electron microscopy and low temperature calorimetry. The w/c specimens (equal to 0.35) cured under sealed conditions first form a depercolated (disconnected) capillary pore system that later reconnects due to self-desiccation and autogenous shrinkage. Conversely, in the w/c specimens (equal to 0.435), there is some indication that sealed curing actually leads to an earlier depercolation of the remaining capillary pores than saturated curing, but without a subsequent repercolation. The results indicate the criticality of proper curing for both w/c specimens, suggesting that curing for strength and curing for durability may require different practices and may provide the impetus for innovative curing strategies to produce concretes with optimum properties.*

**Keywords:** curing; hydration; microstructure; porosity; scanning electron microscopy.

## INTRODUCTION

Proper curing of concrete is widely recognized as a necessity for assuring adequate field performance of concrete structures.<sup>1</sup> Not only is it recognized as important to minimize evaporation of the concrete mixture water, but it is equally emphasized to provide a source of external (or internal) curing water to replace that consumed by chemical shrinkage during the hydration of the cement. A cement paste, mortar, or concrete cured under sealed conditions will self-desiccate, resulting in the creation of coarse capillary pores within the microstructure. For water-cement ratios (w/c) greater than approximately 0.42, there is sufficient water in the mixture such that complete hydration of the cement can be achieved theoretically without supplying additional water to the cement paste.<sup>2</sup> Even if complete hydration were achievable, however, the lack of additional curing water may still result in the creation of relatively large pores within the final microstructure. In this case, the addition of curing water would assure that all pores remain water-filled and eligible as locations for the precipitation and growth of hydration products during curing.

Proper curing of the newer high-performance concretes is both more critical and more difficult.<sup>2</sup> Thus, high-performance concrete has been plagued by ubiquitous early-age cracking problems, and novel solutions, such as the use of internal curing,<sup>3-5</sup> have been developed to avoid or at least reduce such cracking. Early-age cracking is a complex phenomenon, depending on thermally induced strains, autogenous stresses, and strains due to self-desiccation and development of mechanical properties, among others.<sup>6</sup> The microstructure of hydrating cement paste within concrete clearly has a large influence on this phenomenon. Thus, a more fundamental understanding of how this microstructure develops during the course of early hydration, as a function of both w/c and

curing conditions, would assist in optimizing current curing strategies and also in formulating new and innovative ones.

This paper will apply three experimental techniques to characterize the hydration and microstructure of w/c = 0.35 and 0.435 cement pastes cured under saturated and sealed conditions at 20 °C (68 °F) as a function of age. These techniques are loss on ignition (LOI) to estimate the degree of hydration, scanning electron microscopy (SEM) to evaluate the microstructure and the degree of hydration,<sup>7-9</sup> and low temperature calorimetry (LTC) to investigate the developing pore structure in the hydrating cement pastes.<sup>10-14</sup> Specifically, low temperature calorimetry will be used to indicate the connectivity (percolation) of various size pore networks in the hydrating specimens.<sup>10</sup> Igarishi et al.<sup>15</sup> have recently applied SEM analysis to investigate the effect of curing conditions on the development of coarse capillary pores in cement pastes cured under saturated and sealed conditions at temperatures of 20 and 40 °C (68 and 104 °F) for w/c = 0.25, 0.40, and 0.60. They noted that it was extremely difficult to avoid the development of coarse capillary pores in the lowest w/c paste via conventional saturated curing, and also pointed out the critical role of the initial packing of cement particles in influencing the developed microstructure (pore structure).

## RESEARCH SIGNIFICANCE

The concurrent goals of hydration are to connect the original cement particles into as strong a network as possible and to disconnect the original water-filled capillary pore space as much as possible. Understanding the influence of curing practices on this microstructure development is critical to developing rational curing practices and integrating curing into the mixture design process. The experimental program summarized in this paper provides fundamental information to support the criticality of proper curing and to foster innovation in tailoring curing practices to the mixture design, environmental exposure, and desired performance attributes of the in-place concrete.

## EXPERIMENTAL

### Specimen preparation

The cement pastes analyzed in this study were prepared using Cement and Concrete Reference Laboratory (CCRL) portland cement proficiency sample 152,<sup>16</sup> issued in January 2004. Its particle size distribution and phase composition are available online.<sup>17</sup> The cement contained 6% calcium sulfates by volume, distributed as approximately 44% gypsum (calcium sulfate dihydrate), 52% hemihydrate, and 4% anhydrite, as

ACI Materials Journal, V. 103, No. 5, September-October 2006.  
MS No. 05-083 received August 10, 2005, and reviewed under Institute publication policies. Copyright © 2006, American Concrete Institute. All rights reserved, including the making of copies unless permission is obtained from the copyright proprietors. Pertinent discussion including authors' closure, if any, will be published in the July-August 2007 ACI Materials Journal if the discussion is received by April 1, 2007.

ACI member Dale P. Bentz is a Chemical Engineer in the Materials and Construction Research Division, National Institute of Standards and Technology (NIST), Gaithersburg, Md. He received his BS in chemical engineering from the University of Maryland, College Park, Md., in 1984, and his MS in computer and information science from Hood College, Frederick, Md., in 1991. He is a member of ACI Committees 236, Material Science of Concrete, and 308, Curing Concrete. His research interests include the science and technology of building materials, and experimental and computer modeling studies of the microstructure and performance of cement-based and fire-resistant materials.

Paul E. Stutzman is a Physical Scientist in the Materials and Construction Research Division at NIST. He received his AB in geology from Hanover College, Hanover, Ind., in 1980, and an MS in geology from Southern Illinois University at Carbondale, Carbondale, Ill., in 1983. His research interests include the development and application of techniques for characterizing material microstructure.

determined by x-ray diffraction measurements. Cement pastes with initial  $w/c = 0.35$  and  $0.45$  on a mass basis were mixed at  $20^\circ\text{C}$  ( $68^\circ\text{F}$ ) in a temperature-controlled high speed blender using the following protocol: 30 seconds of low speed mixing (4200 rpm) while the cement powder was introduced into the mixing vessel that already contained the water, 30 seconds of high speed mixing (10,000 rpm), a rest of 150 seconds while the sides of the mixing vessel were scraped down, and 30 seconds more of high speed mixing to prepare the final product. Cast wafers ( $\approx 5\text{ g}$  [0.18 oz]) of the prepared pastes, approximately 32 mm (1.26 in.) in diameter and 2 to 5 mm (0.08 to 0.2 in.) in thickness, were placed in small, capped plastic vials to be cured at  $20^\circ\text{C}$  ( $68^\circ\text{F}$ ). After approximately 4 hours of curing, any accumulated bleed water was removed from the vials using a pipette, to assess the true effective  $w/c$  of the pastes. The  $w/c = 0.35$  pastes contained negligible bleed water, but for the  $w/c = 0.45$  pastes, after removing the accumulated bleed water, a paste with an effective  $w/c = 0.435$  remained.

Three curing conditions were employed. In saturated curing, a small amount of distilled water was placed on top of the paste wafers after removing the bleed water. In sealed curing, the wafers were simply sealed in their plastic vials after removal of the bleed water. In sealed/saturated curing, the wafers were cured under sealed conditions for 7 days, then the plastic vials were opened and a small amount of distilled water was added on top of the wafers. All curing was conducted inside of a walk-in environmental chamber maintained at  $20^\circ\text{C}$  ( $68^\circ\text{F}$ ). At various ages between 1 and 256 days, wafers were removed from their vials and crushed into small pieces. Often, some of the small pieces were retained for SEM or LTC analyses as described in the following. The remaining pieces were further crushed to a fine powder, flushed with methanol in a thistle tube under vacuum to stop their hydration, and divided between two crucibles (for replicates) for determination of degree of hydration via LOI measurements.

### Degree of hydration

The nonevaporable water content  $w_n$  of each crucible sample was determined as the mass loss between 105 and  $1000^\circ\text{C}$  ( $221$  and  $1832^\circ\text{F}$ ) divided by the mass of the ignited sample, corrected for the LOI of the unhydrated cement powder, determined in a separate LOI measurement. Previously, the expanded uncertainty in the calculated  $w_n$  has been estimated to be  $0.001\text{ g/g cement}$  ( $0.001\text{ oz/oz cement}$ ), assuming a coverage factor of 2.<sup>18</sup> The values of  $w_n$  were converted to estimated degrees of hydration based on the phase composition of the cement and published coefficients for the nonevaporable water contents of the various cement clinker phases.<sup>19</sup> Based on a propagation of error analysis,

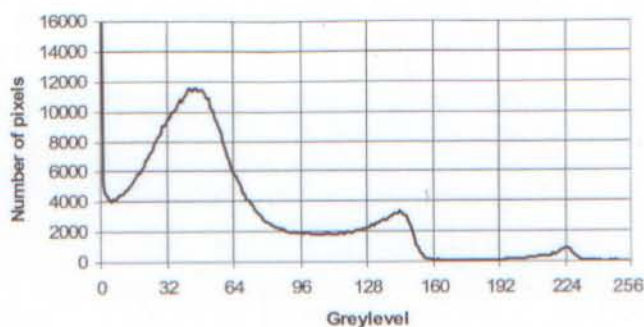


Fig. 1—Graylevel histogram for microstructure image for CCRL Cement 152 with  $w/c = 0.35$ , cured under sealed/saturated conditioned for 92 days.

the estimated uncertainty in the calculated degree of hydration is 0.004.

### Scanning electron microscopy

When the specimens were crushed for the degree of hydration evaluation, small pieces (typically 2 to 3 mm [0.08 to 0.12 in.] in size) were removed and stored in ethanol, to replace the water remaining in the specimens and halt hydration. The pieces were subsequently placed in a low viscosity epoxy to replace the ethanol and cured in an oven at  $60^\circ\text{C}$  ( $140^\circ\text{F}$ ). After curing, the specimens were prepared for viewing at a magnification of  $500\times$  in the SEM as described previously.<sup>20</sup> Four representative images, each with  $1024 \times 768$  pixels, were acquired for the microstructures achieved after 92 days of curing, for both of the  $w/c$  and the three curing conditions investigated in this study. At this magnification, each pixel is approximately  $0.5 \times 0.5\text{ }\mu\text{m}$  ( $2 \times 10^{-5} \times 2 \times 10^{-5}\text{ in.}$ ), with an area of  $0.25\text{ }\mu\text{m}^2$  ( $4 \times 10^{-10}\text{ in.}^2$ ). Each image was analyzed to estimate the area fractions of four components of the hydrated cement paste microstructure: capillary porosity, calcium hydroxide (CH), calcium silicate hydrate gel (C-S-H) along with other hydration products, and unhydrated cement. Based on stereological principles, the two-dimensional area fractions measured in this manner should be equivalent to the three-dimensional volume fractions of the four phases.

To apply a consistent analysis technique to all of the images, the following procedure was employed. A graylevel histogram, such as that shown in Fig. 1, was obtained for each image. This histogram indicates the number of pixels in the image having each possible brightness value (between 0 and 255). For hydrated cement paste, capillary pores are darkest, C-S-H and other (aluminate) hydration products are dark gray, CH is light gray, and unhydrated cement is brightest. The graylevel histogram in Fig. 1 clearly contains several distinct peaks, corresponding to these components of the microstructure. Our goal is to segment (separate) the image into these four components, so that the area (volume) fractions can be determined by simple pixel counting. For separating out the unhydrated cement and the CH, threshold values were selected to be equal to the local minimum between the third and fourth peaks (approximately 180 for the histogram in Fig. 1) and between the second and third peaks (110 for the histogram in Fig. 1) in the graylevel histogram, respectively. To obtain a consistent separation between the C-S-H and the capillary porosity, an alternative procedure to using the local minimum was employed. For a given cement, the volumetric ratio of C-S-H and other

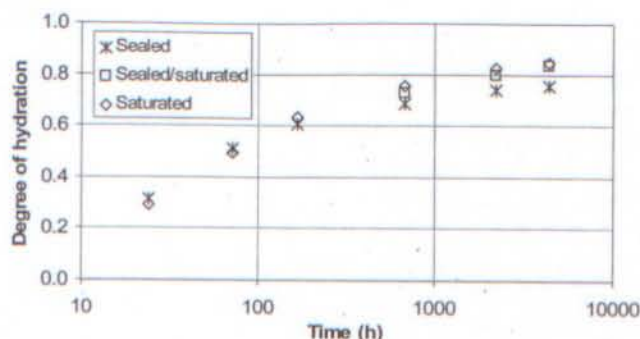


Fig. 2—Degree of hydration via loss on ignition technique versus time for  $w/c = 0.35$  cement paste cured under sealed, sealed/saturated, and saturated curing conditions at  $20^\circ\text{C}$  ( $68^\circ\text{F}$ ).

hydration products to CH should approach a constant value at later ages regardless of curing conditions. Microstructural modeling using the CEMHYD3D hydration model<sup>18,21</sup> has indicated that this value should be approximately 3.7 for CCRL Cement 152. Given the expected image-to-image variation in this quantity for the finite size sample area, a threshold graylevel was chosen to separate the capillary porosity from the C-S-H and other hydration products such that the computed ratio of this quantity was always between 3.58 and 3.82 for the selected threshold.

The degree of hydration of the cement was then estimated according to the equation<sup>7,15</sup>

$$\alpha = \left\{ 1 - \frac{V_{cem}(t)}{V_{cem}(0) \cdot (1 - V_{RS})} \right\} \quad (1)$$

where  $\alpha$  is the computed degree of hydration of the cement;  $V_{cem}(t)$  is the volume (area) fraction of unhydrated cement at time  $t$ ; and  $V_{RS}$  is the initial volume fraction of readily soluble (nonclinker) phases in the cement.

For Cement 152,  $V_{RS} \approx 0.08$ , with 6% calcium sulfates and the remaining 2% corresponding to the alkali sulfates and free lime.  $V_{cem}(0)$  was calculated based on the final  $w/c$  of the prepared pastes, assuming a density of  $3200 \text{ kg/m}^3$  ( $200 \text{ lb/ft}^3$ ) for the powder. These SEM-determined degrees of hydration will be compared to those determined using LOI analysis.

### Low temperature calorimetry

Small pieces of the hydrated cement pastes were also used in the LTC experiments. Sample mass was typically between 30 and 90 mg (0.001 and 0.003 oz). For each LTC experiment, one small piece of the relevant cement paste was surface dried using an absorbent towel and placed in a small open stainless steel pan. The pan with the sample, along with an empty reference pan of similar mass to the empty sample pan, was placed in the calorimeter cell. Using a protocol developed previously,<sup>10</sup> a freezing scan was conducted between 5 and  $-55^\circ\text{C}$  ( $41$  and  $-67^\circ\text{F}$ ) at a scan rate of  $-0.5^\circ\text{C/min}$  ( $-0.9^\circ\text{F/min}$ ). For temperatures between  $-100$  and  $500^\circ\text{C}$  ( $-148$  and  $932^\circ\text{F}$ ), the equipment manufacturer had specified a constant calorimetric sensitivity of  $\pm 2.5\%$  and a root-mean-square baseline noise of  $1.5 \mu\text{W}$ . The peaks observed in a plot of heat flow (normalized to the mass of the sample) versus temperature correspond to water freezing in pores with various size entryways (pore necks). The smaller the

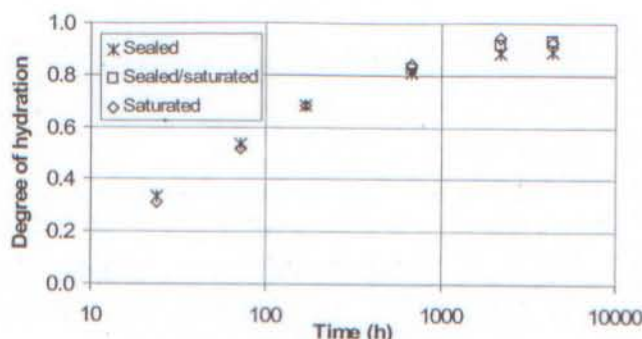


Fig. 3—Degree of hydration via loss on ignition technique versus time for  $w/c = 0.435$  cement paste cured under sealed, sealed/saturated, and saturated curing conditions at  $20^\circ\text{C}$  ( $68^\circ\text{F}$ ).

pore entryway, the more the freezing peak is depressed. Thus, the presence of, absence of, or change in peaks can be used to infer information concerning the characteristic sizes of the percolated (connected) water-filled pores in the microstructure of the hydrating cement pastes. One advantage of LTC over mercury intrusion porosimetry, and other techniques for assessing pore size and connectivity, is that specimens are evaluated without any drying that might damage the pore structure. Of course, the LTC technique can only assess the size and connectivity of water-filled pores. For nonsaturated curing conditions, it is assumed that empty pores formed due to self-desiccation will not contain any freezable water and thus will not show up on the LTC scans.

## RESULTS

### Degree of hydration

The degrees of hydration measured using the LOI technique are summarized in Fig. 2 and 3, for the  $w/c = 0.35$  and  $w/c = 0.435$  cement pastes, respectively. Three major observations can be taken from the figures. First, a higher degree of hydration is ultimately achieved in the  $w/c = 0.435$  pastes, due both to their higher water content and to the presence of more space available for the precipitation and growth of hydration products. Second, for both  $w/c$  values, sealed curing results in a lower degree of hydration at later ages.<sup>22</sup> As would be expected, this decrease is more significant for the lower  $w/c$  cement paste. Third, in terms of achieved degree of hydration, the sealed/saturated curing condition, in which the cement pastes were cured under sealed conditions for 7 days and then saturated on top, appears to provide equivalent performance to the saturated curing condition for the thin cement paste specimens employed in this study. Any differences between the saturated and the sealed/saturated curing condition results are well within the experimental error ( $\pm 0.004$ ) in the LOI technique. This third observation leads to the natural question: does equivalency in achieved degree of hydration correspond to equivalency in the microstructure developed during that (globally equal) amount of hydration? The answer is provided in the SEM and LTC analyses to be presented in the following.

### Scanning electron microscopy

Typical processed SEM micrographs for the  $w/c = 0.35$  and  $0.435$ , 92-day cement pastes are provided in Fig. 4 and 5, respectively. In the figures, unhydrated cement particles are white, calcium hydroxide is light gray, C-S-H and other

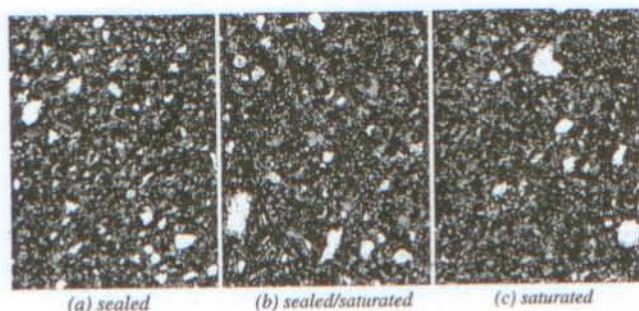


Fig. 4—92-day segmented SEM microstructures for  $w/c = 0.35$  cement pastes.

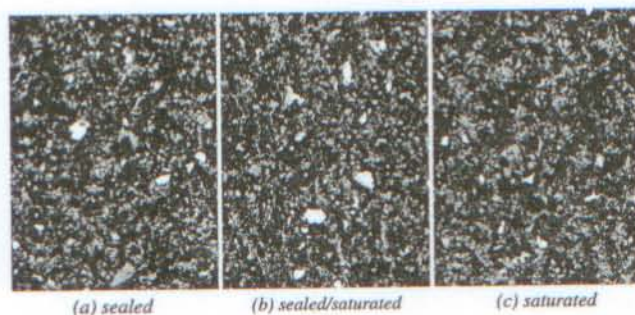


Fig. 5—92-day segmented SEM microstructures for  $w/c = 0.435$  cement pastes.

hydration products are dark gray, and capillary pores are black. A large influence of curing conditions on the hydrated microstructures is observed. For hydration under sealed conditions, there exists a set of large (empty) capillary pores ( $10 \mu\text{m}^2$  [ $1.6 \times 10^{-8} \text{ in.}^2$ ] and larger) for both  $w/c$  systems. These pores are present due to the chemical shrinkage and self-desiccation occurring during hydration, as the largest pores are observed to be the first to empty during either internal or external drying at early ages.<sup>22,23</sup> For saturated and sealed/saturated curing, there are fewer of these large pores, although they are not eliminated entirely. For these saturated curing conditions, more and coarser pores are observed in the  $w/c = 0.435$  system, due to the larger initial spacing (and thus pore size) between cement particles.<sup>15,24</sup>

A quantitative analysis of the coarse porosity was performed by determining the size of each individual two-dimensional pore in the SEM images. Histograms of the obtained pore areas (in pixels) are provided in Fig. 6, for the  $w/c = 0.35$  pastes. The area fractions of the microstructures occupied by pores larger than 30 pixels or  $7.5 \mu\text{m}^2$  ( $1.2 \times 10^{-8} \text{ in.}^2$ ) are provided in Table 1. For both  $w/c$  specimens, curing under saturated conditions resulted in the least remaining volume of coarse pores after 92 days, followed by curing under sealed/saturated conditions, and finally by sealed conditions. While curing under saturated or sealed/saturated conditions resulted in basically the same achieved degrees of hydration (Fig. 2 and 3), in the latter case, there is a significantly higher volume fraction occupied by the coarse pores. Many of these pores would have been created due to chemical shrinkage during the initial 7 days of sealed curing, and these results suggest that they are only partially filled in by reaction products after additional curing water is provided and hydration continues. While the size and number of these pores should certainly influence the mechanical properties of these materials, it is more likely that their connectivity (percolation)

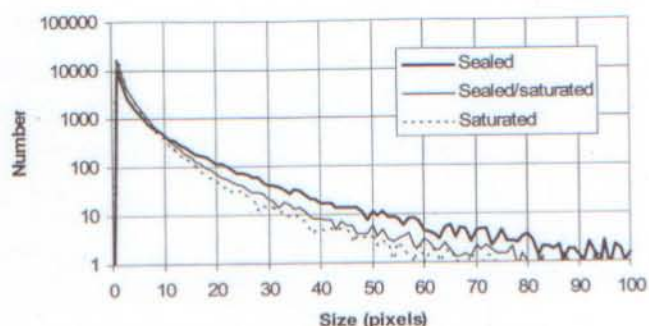


Fig. 6—Two-dimensional pore size distribution for  $w/c = 0.35$  cement paste cured for 92 days under three different curing conditions.

Table 1—Fraction of cement paste volume occupied by capillary pores larger than  $7.5 \mu\text{m}^2$  ( $1.2 \times 10^{-8} \text{ in.}^2$ ) (in two dimensions) and measured degrees of hydration for cement pastes cured for 92 days

$w/c$	Curing	Coarse porosity fraction	$\alpha_{SEM}$	$\alpha_{LOI}$
0.35	Sealed	0.050	$0.80 \pm 0.014$	$0.74 \pm 0.004$
0.35	Sealed/saturated	0.019	$0.85 \pm 0.016$	$0.80 \pm 0.004$
0.35	Saturated	0.011	$0.87 \pm 0.031$	$0.82 \pm 0.004$
0.435	Sealed	0.042	$0.93 \pm 0.003$	$0.88 \pm 0.004$
0.435	Sealed/saturated	0.022	$0.95 \pm 0.012$	$0.92 \pm 0.004$
0.435	Saturated	0.014	$0.96 \pm 0.015$	$0.94 \pm 0.004$

characteristics will influence the transport properties and durability. The results to be presented in the LTC section to follow will explore these percolation aspects in detail.

As indicated by the results tabulated in Table 1, the degrees of hydration determined for the various cement pastes via the SEM analysis are consistently slightly higher (approximately 0.05) than those determined by the LOI technique. This could be due to the presence of very small unhydrated cement particles that would not be identifiable in the SEM images. The rank order for the different  $w/c$  values and different curing conditions, however, is the same for both techniques.

### Low temperature calorimetry

Initially, LTC analyses were conducted on only the most well hydrated (182 days and beyond) samples of the different cement pastes. Typical results for the  $w/c = 0.35$  and 0.435 pastes are provided in Fig. 7 and 8, respectively. Sealed/resat refers to a specimen that was cured under sealed conditions, then resaturated by placing in an excess of lime-saturated water (typically for 1 day) prior to the LTC measurement. As can be seen in Fig. 7 and 8, a single LTC scan produces a graph of heat flow versus temperature that consists of a baseline and one or more peaks at specific temperatures. Each peak corresponds to water freezing in a set of pores with an entryway pore diameter determined by the freezing point depression.<sup>25</sup> Adopting the naming convention of Snyder and Bentz,<sup>10</sup> the three most commonly occurring peaks are referred to as corresponding to capillary pores freezing at approximately  $-15^\circ\text{C}$  ( $5^\circ\text{F}$ ), open gel pores freezing between approximately  $-25$  and  $-30^\circ\text{C}$  ( $-13$  and  $-22^\circ\text{F}$ ), and dense gel pores freezing between approximately  $-40$  and  $-45^\circ\text{C}$  ( $-40$  and  $-49^\circ\text{F}$ ). While only a coarse approximation, using the techniques outlined by

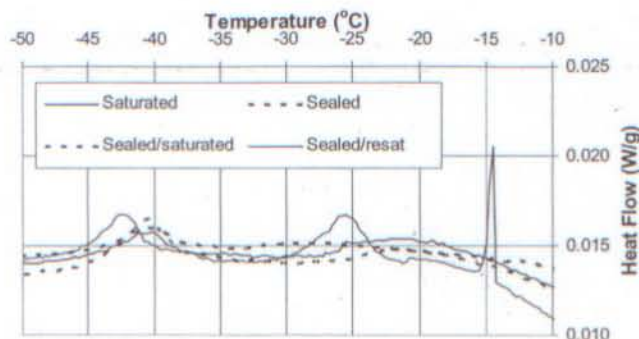


Fig. 7—LTC results for CCRL Cement 152,  $w/c = 0.35$  pastes, cured for 228 days.

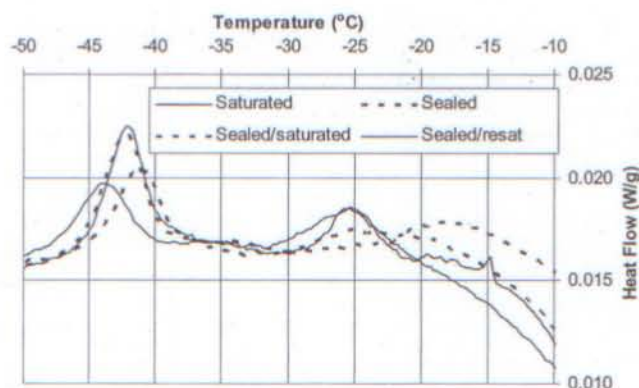


Fig. 8—LTC results for CCRL Cement 152,  $w/c = 0.435$  pastes, cured for 214 days.

Fagerlund,<sup>25</sup> these three freezing temperatures would correspond to pore radii of approximately 10, 6, and 4.5 nm ( $4 \times 10^{-7}$ ,  $2.4 \times 10^{-7}$ , and  $1.8 \times 10^{-7}$  in.), respectively. These pore radii are provided only as rough guides, as the freezing point depression is influenced by the ionic concentration of the (freezing) pore solution in addition to the size of the assumed cylindrical pore entryways.<sup>14</sup>

As proposed by Snyder and Bentz,<sup>10</sup> the presence or absence of the  $-15^\circ\text{C}$  ( $5^\circ\text{F}$ ) peak apparently indicates the percolation state of the capillary porosity within the hydrating cement paste. A percolated set of capillary-size pores will dramatically increase the permeability of the material<sup>26</sup> and also directly influence its freezing-and-thawing durability, as the water in these coarser connected pores will be the first (and perhaps the only water) to freeze during exposure to low temperature weather conditions. In general, lower  $w/c$  pastes require less hydration to achieve depercolation of capillary pores than higher  $w/c$  pastes. For ordinary portland cement pastes with  $w/c > 0.5$ , depercolation may not be possible even at complete hydration because sufficient capillary porosity remains to form a percolated network through the three-dimensional microstructure.<sup>26,27</sup> For the  $w/c = 0.35$  pastes (Fig. 7), the only indication of a highly percolated capillary pore system was found for a specimen first cured under sealed conditions for 228 days and then resaturated (for 3 days) prior to the LTC measurement. This specimen exhibited peaks corresponding to both capillary and open gel porosity that were not observed for any of the three originally applied curing conditions. The most likely explanation is that the  $w/c = 0.35$  specimen cured under sealed conditions developed a connected (but empty)

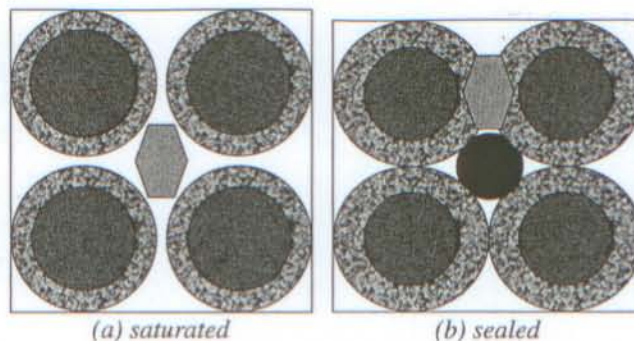


Fig. 9—Four-particle model for hydrating cement paste microstructure, indicating hydration under saturated and sealed curing conditions. Dark gray is unhydrated cement grains, textured material and light gray are hydration products, white is water-filled porosity, and black is empty porosity.

network of these pores, which became water-filled (and only then detectable by LTC) during resaturation. This network of connected pores would likely include the extremely coarse pores visible for the specimen cured under sealed conditions in Fig. 4(a). The question remains as to whether these connected coarse pores were present throughout the hydration under sealed conditions or whether they depercolated initially due to hydration and later reopened and repercolated due to shrinkage of the C-S-H during self-desiccation, similar to the depercolation/repercolation observed by Bager and Sellevold<sup>12,13</sup> during the drying/resaturation of well hydrated cement pastes. Answering this question required further LTC experiments described in the following.

In general, for the  $w/c = 0.435$  pastes (shown in Fig. 8), as would be expected, a coarser percolated (open gel and capillary) pore structure was present for all three curing conditions, as indicated by the peaks at  $-15^\circ\text{C}$  and  $-25^\circ\text{C}$  ( $5^\circ\text{F}$  and  $-13^\circ\text{F}$ ). Surprisingly, the specimen cured under saturated conditions exhibited the most evidence of percolated capillary pore (small peak at  $-15^\circ\text{C}$  [ $5^\circ\text{F}$ ]) and percolated open gel pore structures. The sealed/saturated curing and the sealed curing specimen that was resaturated after 214 days both exhibited a much larger volume of the dense gel pores, suggesting that the capillary pores and many of the open gel pores had depercolated under these curing procedures and were thus only detectable as part of the dense gel pores (similar to the well known ink-bottle effect in mercury intrusion porosimetry). This is rather surprising in that it suggests that in terms of depercolating the capillary porosity to reduce the permeability and increase the durability of the cement paste, sealed curing may be superior to saturated curing, at least for the thin  $w/c = 0.435$  paste specimens examined in this study. To understand why this could be so, it is helpful to introduce a simple four-particle model for the hydrating cement paste microstructure.

Such a model is provided in Fig. 9, which shows four cement particles hydrating under either saturated or sealed curing conditions. For saturated curing, all of the capillary porosity remains water-filled and accessible to the growing hydration products, which may form around the original cement grains or in the capillary pore space between particles, as illustrated in Fig. 9(a). When curing for maximum strength, this may represent the ideal curing, as the degree of hydration will be maximized and no large empty self-desiccation pores will form. For sealed curing, such empty pores will

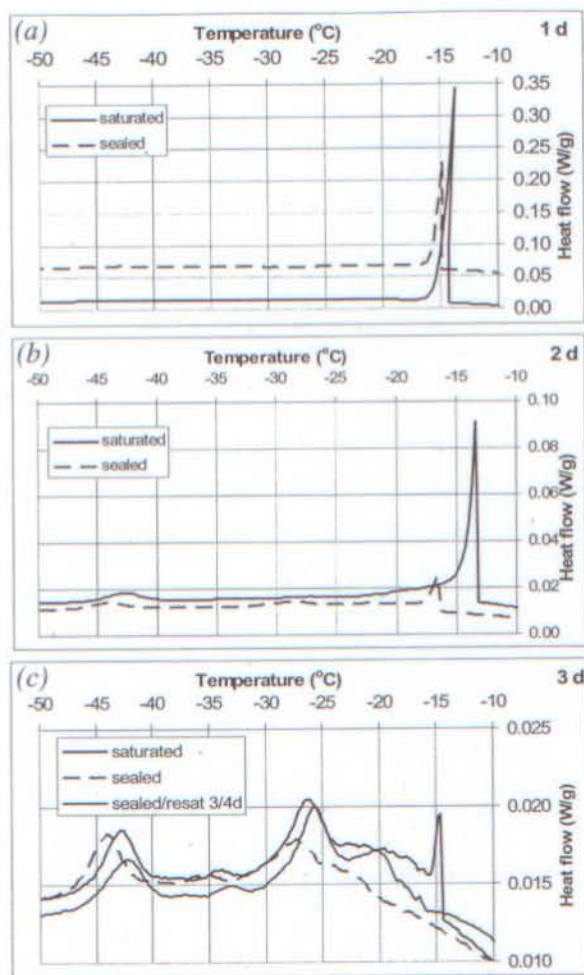


Fig. 10—LTC scans for  $w/c = 0.35$  cement pastes cured for: (a) 1 day; (b) 2 days; and (c) 3 days. Note y-axis scales are different. Sealed/resat specimen indicates time of sealed curing (3 days) followed by time at which LTC measurement was performed (4 days) after subsequent (re)saturated curing.

indeed form in the largest available water-filled spaces, as illustrated by the centrally located empty pore in Fig. 9(b), and the growing hydration products will thus be limited to forming in the remaining water-filled pore spaces. This will tend to concentrate the hydration product formation in the smaller pore entryways between particles as shown in Fig. 9(b), where it will be the most efficient in depercolating the connected capillary pore network, and thus this may be the preferred curing procedure for optimizing performance with respect to permeability and durability. Note that under sealed curing conditions in Fig. 9(b), the four pore entryways between particles are disconnected by the hydration products, while they remain connected under the saturated curing conditions in Fig. 9(a). Previously, both Swayze<sup>28</sup> and Powers<sup>29</sup> have suggested that sealed curing for a short period of time prior to application of curing water could be beneficial for both short term (thermal cracking<sup>28</sup>) and long term (frost action<sup>29</sup>) concrete durability in some cases. The simple model in Fig. 9 would support the experimental observation that for the  $w/c = 0.435$  pastes, the capillary and open gel porosities are depercolated to a greater extent for the sealed and sealed/saturated curing procedures than for the saturated curing. Obviously, this did not hold true for the  $w/c = 0.35$  pastes, where a coarse percolated pore network developed in

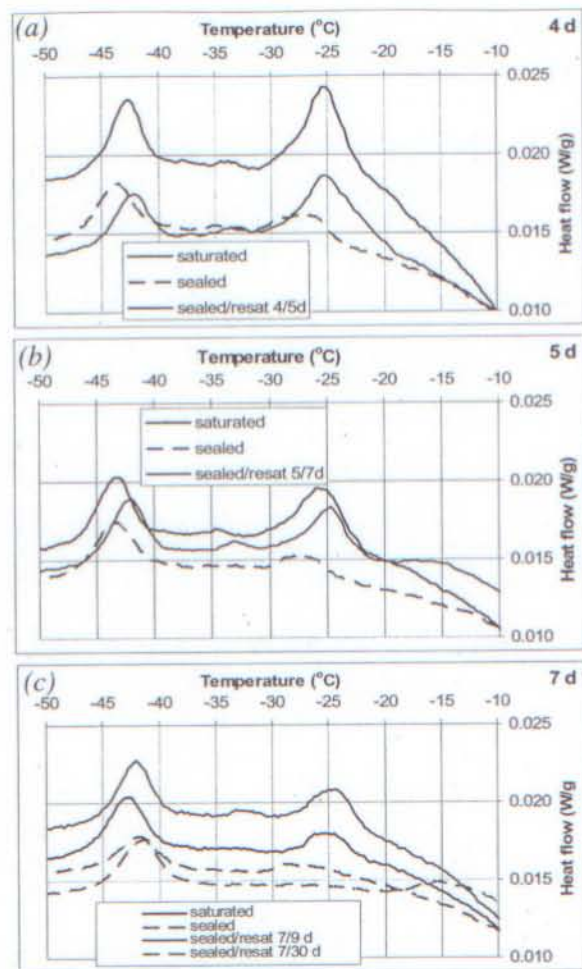


Fig. 11—LTC scans for  $w/c = 0.35$  cement pastes cured for: (a) 4 days; (b) 5 days; and (c) 7 days.

the paste cured under sealed conditions for 228 days (Fig. 7). Further LTC experiments were conducted to elucidate the differences between these two  $w/c$  pastes.

Cement pastes were prepared as before with  $w/c = 0.35$  and LTC scans were conducted at more frequent intervals beginning at an age of 1 day. Saturated, sealed, and sealed/saturated curing conditions were again investigated, but the amount of sealed curing time before resaturating the specimens was varied, unlike the constant 7 day value used in the first experiments. Results are shown in Fig. 10, 11, and 12 for early (1 to 3 days), middle (4 to 7 days), and late (14 to 50 days) ages, respectively. At the earliest ages of 1 and 2 days, shown in Fig. 10, the dominant feature in the LTC scans for both saturated and sealed curing conditions is a large peak corresponding to connected capillary porosity. For both ages, the area under this peak is considerably less for the sealed specimens, in agreement with the self-desiccation occurring in these specimens relative to the water imbibition occurring in those cured under saturated conditions. At 3 days, in Fig. 10, the formation of the open gel and dense gel connected pore structures at the expense of the connected capillary pore system can be clearly observed, suggesting that the capillary pore entryways are being filled by gel hydration products, as shown in Fig. 9(b).

As the hydration proceeds to 4, 5, and 7 days, the capillary pore peak is no longer observed in any of the LTC scans in Fig. 11. At 4 days, a large open gel porosity peak exists; this

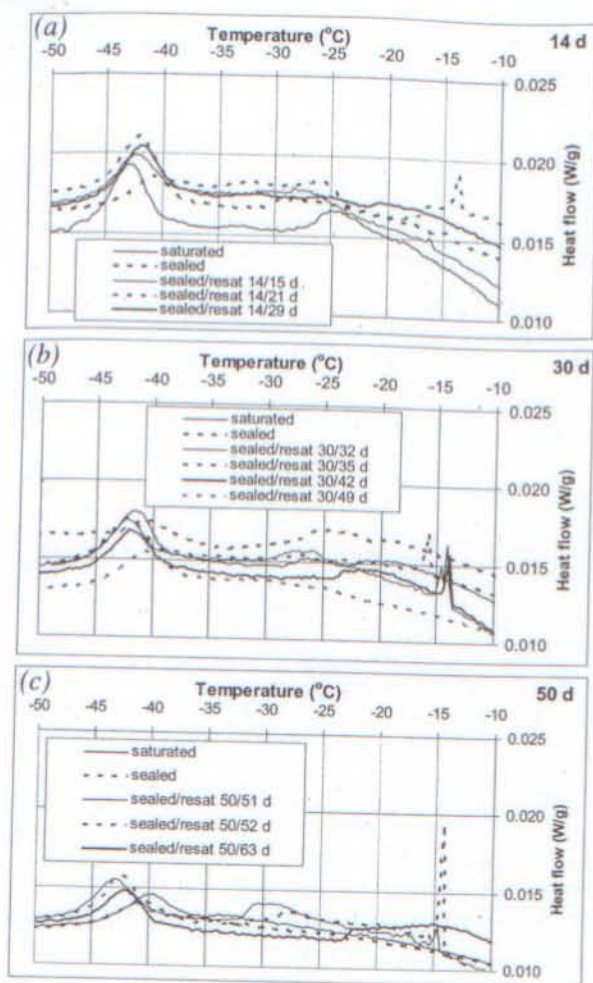


Fig. 12—LTC scans for  $w/c = 0.35$  cement pastes cured for: (a) 14 days; (b) 30 days; and (c) 50 days.

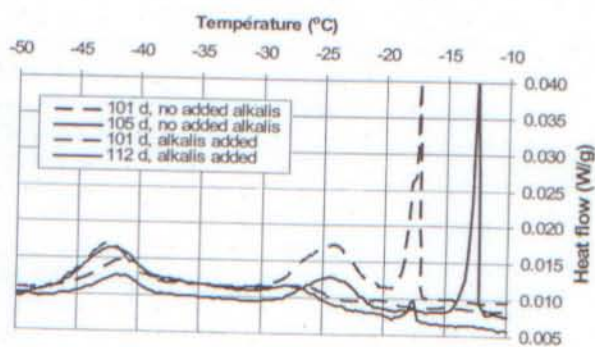


Fig. 13—Influence of added alkalis on percolation of capillary porosity in CCRL Cement 140 pastes with  $w/c = 0.4$  hydrated under saturated curing conditions.

detected as part of the dense gel network. These LTC scans would suggest a less permeable, more durable cement paste microstructure. The findings do not end here.

Proceeding to the later age hydration results shown in Fig. 12, perhaps surprisingly, the coarsest capillary pore peak reappears. For the  $w/c = 0.35$  paste, once the capillary porosity depercolates, self-desiccation will occur to some level in the hydrating microstructure, even in the specimens cured under saturated conditions. Significant autogenous shrinkage stresses will be created; the smaller the pores being emptied by self-desiccation, the greater the autogenous stresses and strains created in the three-dimensional microstructure.<sup>24</sup> Thus, these stresses and their accompanying shrinkage strains can be much greater in the  $w/c = 0.35$  cement paste, as it initially contains smaller pores than the  $w/c = 0.435$  cement paste, due to the closer packing of the cement particles.<sup>15,24</sup> While lower  $w/c$  pastes would be expected to have higher values of elastic modulus, in practice, the autogenous stresses are higher, so that the measured autogenous shrinkage strain increases as the  $w/c$  decreases.<sup>30</sup> As the gel shrinks, the pore entryways that were first depercolated by the gel growing during hydration may now become repercolated by the gel shrinking (like a wet sponge drying around a golf ball) during internal drying. This would result in the microstructure changing from one similar to that shown in Fig. 9(b) to one similar to that shown in Fig. 9(a), assuming that the cement particle cores remained in their original (fixed) locations. These observations are consistent with those of Bager and Sellevold concerning the drying and resaturation of room temperature cured cement pastes.<sup>12,13</sup> They observed that, upon drying and resaturation, coarse connected capillary pores reappeared in the cement paste microstructures. While they imposed reduced relative humidities on their specimens via external drying, here, the internal relative humidity is reduced autogenously due to the chemical shrinkage and self-desiccation accompanying the cement hydration reactions.<sup>24,31,32</sup> It should be noted that for sealed curing conditions, microcrack formation could also be contributing to the observed repercolation of the open gel and capillary pores.

It is interesting to consider the ramifications of this repercolation of the capillary pore network for the distinct cases of sealed and saturated curing. In sealed curing, as the gel shrinks and the pores reopen, they will basically remain filled with air (or water vapor). As the shrinkage continues and the autogenous stresses intensify with any further hydration, the pores will become even more connected, as exemplified by the presented sealed/resaturated LTC scans for the 14, 30, and 50 days sealed curing regimens in Fig. 12. Thus, by 228 days, as shown for the sealed/resaturated specimen in Fig. 7, both the open gel and capillary pore structures are highly percolated. Conversely, for saturated curing of the small specimens used in this study, as the pores repercolate, the permeability of the paste will increase and water will be more easily imbibed from the exterior to refill the empty pores. With continuing hydration and water (re)absorption (and possibly swelling) by the shrunken gel, the capillary pores may depercolate once again, starting the depercolation/repercolation cycle all over again. In this manner, the behavior of the material would be somewhat analogous to a pump, as a suction potential would be periodically created and satiated within the hydrating microstructure, all the while pumping in external curing water. Thus, the  $w/c = 0.35$  specimens cured for 228 days

unc  
por  
co  
anc  
A  
lov  
mu  
pas  
not  
so  
Fu  
in  
hy  
arc  
pre  
cu  
As  
sh  
be  
be  
alt  
es  
mi  
ex  
co  
ma  
on  
  
co  
sr  
of  
pr  
tha  
ha  
ge  
wi  
co  
ca  
bu  
the  
hi  
str  
of  
so  
  
m:  
ca  
fo  
a  
co  
pc  
fo  
all  
de  
di  
bc  
  
fr  
of  
or  
of  
pc  
•

under saturated conditions exhibit primarily only a dense gel porosity peak in the LTC scan (Fig. 7) and there are very few coarse pores present in the hydrated microstructure (Fig. 4(c) and Table 1).

Whether this behavior would hold for a  $w/c$  significantly lower than 0.35 is unknown at this time. With the initially much denser particle packings in these lower  $w/c$  cement pastes, the initial depercolation of the capillary porosity may not be easily overcome by subsequent shrinkage of the C-S-H, so that the coarse capillary pore network may not re-percolate. Furthermore, the shrinkage stresses will be even higher than in the  $w/c = 0.35$  cement paste, so that the C-S-H and other hydration products may shrink tightly (like shrink wrap) around the unhydrated cement particles, effectively preventing further hydration of the particles even if additional curing water were to be imbibed into the microstructure.<sup>29</sup> As with drying shrinkage, a portion of this autogenous shrinkage is likely irreversible, as new chemical bonds will be created within the C-S-H nanostructure.<sup>33</sup> In this case, the best curing approach might be to avoid the self-desiccation altogether or at least reduce it by the use of internal curing,<sup>3-5</sup> especially considering the increased propensity for extensive microcracking and possibly macrocracking damage in extremely low  $w/c$  mixtures cured under nonsaturated conditions. The best efforts to create a low permeability material will be totally compromised if the pore structure is only depercolated between percolated cracks.

As always, numerous complicating factors arise when considering the extension of these experimental results on small cement paste specimens in the laboratory to the curing of concrete structures in the field. One such factor is the presence of interfacial transition zones (ITZs) in concrete that are not found in the cement paste specimens. These ITZs have a higher effective  $w/c$  than the bulk cement paste and generally contain more and larger capillary pores. Thus, they will often be the first to empty during self-desiccation<sup>34</sup> and could easily constitute their own percolated network of capillary pores, compromising the low permeability of the bulk cement paste. With this in mind, it is not surprising that the permeability of concrete can be two orders of magnitude higher than that of comparable cement paste.<sup>35</sup> The microstructure of the ITZ can be densified, however, by the addition of silica fume or other fine pozzolanic or hydraulic materials,<sup>36</sup> so that this weak link may be effectively removed.

The shrinkage/swelling of the C-S-H gel seems to have major implications for the depercolation/repercolation of the capillary porosity in hydrating cement paste. Further support for this can be found in the LTC scans shown in Fig. 13, for a  $w/c = 0.4$  CCRL Cement 140<sup>17</sup> paste cured under saturated conditions, with and without the incorporation of additional potassium and sodium sulfates in the mixture. After curing for approximately 100 days, clearly the paste with the added alkalis exhibits a pore structure that is substantially more depercolated than the paste with no additional alkalis. This difference in pore structure would be expected to influence both the transport and mechanical properties of the mixtures.

To summarize, based on the microstructural observations from hydrating cement pastes, optimum curing is a function of the  $w/c$ , as well as whether curing is to optimize strength or permeability/durability. The following is a preliminary set of recommendations based on the present study for ordinary portland cement-based materials:

- Very low  $w/c$  ( $\leq 0.35$ )—internal curing may be needed when it is desirable to avoid self-desiccation, autogenous

stresses and strains, and their accompanying local damage (repercolation) to the hydrating cement paste microstructure;

- Low  $w/c$  (0.35 to 0.4)—internal or external curing may be a viable option, but saturation of the hydrating cement paste should be maintained as long as possible;
- Intermediate  $w/c$  (0.4 to 0.45)—sealed/saturated curing may be a viable option when curing for durability; otherwise, external saturated curing should be adequate; and
- High  $w/c$  ( $>0.45$ ): it will likely be very difficult to depercolate the pore structure regardless of the curing practice employed.

In the latter case, if  $w/c$  is close to 0.45, it may be possible to depercolate the pore system by the addition of modest amounts of silica fume or other fine fillers. These materials further refine the pore structure and lead to an earlier depercolation of the capillary pore structure, as evidenced by the LTC results of Villadsen.<sup>37</sup> In general, addition of silica fume or other fine materials that aid in depercolation of the pores would shift all of the aforementioned recommendations to a higher  $w/c$ . For example, in these blended systems, internal curing may be a necessity for all water-solids ratio ( $w/s$ )  $< 0.40$ . In higher  $w/c$  residential concretes, as suggested by Hooton,<sup>38</sup> the best approach to increasing durability may be to add a moderate amount of these fine particles and pay appropriate attention to curing details.

## CONCLUSIONS

The influence of curing on both global hydration and local microstructure has been highlighted. Low temperature calorimetry has been shown to be particularly effective in understanding the developing pore structure in hydrating cement pastes. The connectivity of these pores is strongly influenced by the  $w/c$ , curing conditions, and the alkali content of the cement, and in turn will dramatically impact the permeability, resistance to freezing and thawing, and overall durability of the final concrete. Curing for strength and curing for durability may require different curing practices to promote development of the microstructural features that are most beneficial in each case: low porosity with small pores and a discontinuous capillary pore network, respectively. Preliminary recommendations for curing have been provided, ranging from the recently implemented usage of internal curing, through conventional external curing, to a seemingly counterintuitive procedure of sealed/saturated curing. Each has the potential for optimizing the performance of a different class of concrete and the field practitioners will surely determine the viability and range of applicability of each approach over the years to come.

## ACKNOWLEDGMENTS

The authors would like to thank M. Peltz of the Building and Fire Research Laboratory (BFRL) at NIST for measuring the particle size distribution of the cement powder, K. Snyder (BFRL) for useful conversations and suggestions, and N. Carino (BFRL) for a thorough review of the manuscript.

## NOTATION

CH	=	calcium hydroxide
C-S-H	=	calcium silicate hydrate gel
ITZ	=	interfacial transition zone
LOI	=	loss on ignition
LTC	=	low temperature calorimetry
SEM	=	scanning electron microscopy
$t$	=	time, hours
$V_{cem}(t)$	=	volume fraction of cement at time $t$
$V_{RS}$	=	volume fraction of readily soluble (nonclinker) phases in initial cement

w/c = water-cement ratio  
 w/s = water-solids ratio  
 $w_n$  = nonevaporable water content of cement paste  
 $\alpha$  = degree of hydration of cement paste

## REFERENCES

1. ACI Committee 308, "Guide to Curing Concrete (ACI 308R-01)," American Concrete Institute, Farmington Hills, Mich., 2001, 31 pp.
2. Meeks, K. W., and Carino, N. J., "Curing of High-Performance Concrete: Report of the State-of-the-Art," NISTIR 6295, U.S. Department of Commerce, Mar. 1999.
3. Philleo, R. E., "Concrete Science and Reality," *Materials Science of Concrete II*, J. Skalny and S. Mindess, eds., American Ceramic Society, Westerville, Ohio, 1991, pp. 1-8.
4. Bentz, D. P.; Geiker, M. R.; and Jensen, O. M., "On the Mitigation of Early Age Cracking," *Self-Desiccation and Its Importance in Concrete Technology III*, B. Persson and G. Fagerlund, eds., Lund Institute of Technology, Lund, Sweden, 2002, pp. 195-203.
5. Geiker, M. R.; Bentz, D. P.; and Jensen, O. M., "Mitigating Autogenous Shrinkage by Internal Curing," *High-Performance Structural Lightweight Concrete*, SP-218, J. P. Ries and T. A. Holm, eds., American Concrete Institute, Farmington Hills, Mich., 2004, pp. 143-154.
6. Bentz, D. P., and Jensen, O. M., "Mitigation Strategies for Autogenous Shrinkage Cracking," *Cement and Concrete Composites*, V. 26, No. 6, 2004, pp. 677-685.
7. Feng, X.; Garboczi, E. J.; Bentz, D. P.; Stutzman, P. E.; and Mason, T. O., "Estimation of the Degree of Hydration of Blended Cement Pastes by a Scanning Electron Microscope Point-Counting Procedure," *Cement and Concrete Research*, V. 34, 2004, pp. 1787-1793.
8. Kjellsen, K. O., and Fjallberg, L., "Measurements of the Degree of Hydration of Cement Paste by SEM,  $^{29}\text{Si}$  NMR and XRD Methods," *Proceedings of the Workshop on Water in Cement Paste & Concrete Hydration and Pore Structure*, Skagen, Denmark, The Nordic Concrete Federation, 1999, pp. 85-98.
9. Scrivener, K. L.; Patel, H. H.; Pratt, P. L.; and Parrott, L. J., "Analysis of Phases in Cement Paste Using Backscattered Electron Images, Methanol Adsorption and Thermogravimetric Analysis," *Materials Research Society Symposium Proceedings*, V. 85, 1987, pp. 67-76.
10. Snyder, K. A., and Bentz, D. P., "Suspended Hydration and Loss of Freezable Water in Cement Pastes Exposed to 90% Relative Humidity," *Cement and Concrete Research*, V. 34, 2004, pp. 2045-2056.
11. Bager, D. H., and Sellevold, E. J., "Ice Formation in Hardened Cement Paste, Part I—Room Temperature Cured Pastes with Variable Moisture Contents," *Cement and Concrete Research*, V. 16, 1986, pp. 709-720.
12. Bager, D. H., and Sellevold, E. J., "Ice Formation in Hardened Cement Paste, Part II—Drying and Resaturation on Room Temperature Cured Pastes," *Cement and Concrete Research*, V. 16, 1986, pp. 835-844.
13. Bager, D. H., and Sellevold, E. J., "Ice Formation in Hardened Cement Paste, Part III—Slow Resaturation of Room Temperature Cured Pastes," *Cement and Concrete Research*, V. 17, 1987, pp. 1-11.
14. Setzer, M. J., "Interaction of Water with Hardened Cement Paste," *Ceramic Transactions: Advances in Cementitious Materials*, V. 16, S. Mindess, ed., American Ceramic Society, Westerville, Ohio, 1992, pp. 415-439.
15. Igarashi, S.; Watanabe, A.; and Kawamura, M., "Effects of Curing Conditions on the Evolution of Coarse Capillary Pores in Cement Pastes," *PRO36: Proceedings of the International RILEM Symposium On Concrete Science & Engineering—A Tribute to Arnon Benur*, K. Kovler, J. Marchand, S. Mindess, and J. Weiss, eds., RILEM Publications S.A.R.L., Paris, France, 2004.
16. Cement and Concrete Reference Laboratory, "Cement and Concrete Reference Laboratory Proficiency Sample Program: Final Report on Portland Cement Proficiency Samples Number 151 and 152," Gaithersburg, Md., Apr. 2004, available at <http://www.ccril.us>.
17. PSDs and Phase Compositions for CCRL Proficiency Cement Samples 140 and 152, available at <http://ciks.cbt.nist.gov/bentz/phpcrl/database/images/>.
18. Bentz, D. P., "Three-Dimensional Computer Simulation of Cement Hydration and Microstructure Development," *Journal of the American Ceramic Society*, V. 80, No. 1, 1997, pp. 3-21.
19. Molina, L., "On Predicting the Influence of Curing Conditions on the Degree of Hydration," *CBI Report 5:92*, Swedish Cement and Concrete Research Institute, Stockholm, Sweden, 1992.
20. Bentz, D. P., and Stutzman, P. E., "SEM Analysis and Computer Modeling of Hydration of Portland Cement Particles," *Petrography of Cementitious Materials*, ASTM STP 1215, S. M. DeHayes and D. Stark, eds., ASTM International, West Conshohocken, Pa., 1994, pp. 60-73.
21. Bentz, D. P., "CEMHYD3D: A Three-Dimensional Cement Hydration and Microstructure Development Modelling Package, Version 2.0," NISTIR 6485, U.S. Department of Commerce, Apr. 2000.
22. Bentz, D. P.; Snyder, K. A.; and Stutzman, P. E., "Microstructural Modeling of Self-Desiccation During Hydration," *Self-Desiccation and Its Importance in Concrete Technology*, B. Persson and G. Fagerlund, eds., Lund Institute of Technology, Lund, Sweden, 1997, pp. 132-140.
23. Bentz, D. P.; Hansen, K. K.; Madsen, H. D.; Vallee, F. A.; and Griesel, E. J., "Drying/Hydration in Cement Pastes During Curing," *Materials and Structures*, V. 34, 2001, pp. 557-565.
24. Bentz, D. P.; Jensen, O. M.; Hansen, K. K.; Oleson, J. F.; Stang, H.; and Haecker, C. J., "Influence of Cement Particle Size Distribution on Early Age Autogenous Strains and Stresses in Cement-Based Materials," *Journal of the American Ceramic Society*, V. 84, 2001, pp. 129-135.
25. Fagerlund, G., "Determination of Pore-Size Distribution from Freezing-Point Depression," *Matériaux et Constructions*, V. 6, No. 33, 1973, pp. 215-225.
26. Powers, T. C.; Copeland, L. E.; and Mann, H. M., "Capillary Continuity or Discontinuity in Cement Paste," *PCA Bulletin*, V. 10, 1959, pp. 2-12.
27. Bentz, D. P., and Garboczi, E. J., "Percolation of Phases in a Three-Dimensional Cement Paste Microstructural Model," *Cement and Concrete Research*, V. 21, No. 2, 1991, pp. 325-344.
28. Swayze, M. A., "Early Concrete Volume Changes and Their Control," *ACI Journal, Proceedings* V. 39, No. 5, 1942, pp. 425-440.
29. Powers, T. C., "A Discussion of Cement Hydration in Relation to the Curing of Concrete," *Proceedings of the Highway Research Board*, V. 27, 1947, pp. 178-188.
30. Tazawa, E., and Miyazawa, S., "Influence of Cement and Admixture on Autogenous Shrinkage of Cement Paste," *Cement and Concrete Research*, V. 25, No. 2, 1995, pp. 281-287.
31. Gause, G. R., and Tucker Jr., J., "Method For Determining the Moisture Condition in Hardened Concrete," *Journal of Research of the National Bureau of Standards*, V. 25, 1940, pp. 403-416.
32. Jensen, O. M., and Hansen, P. F., "Autogenous Deformation and Change of the Relative Humidity in Silica Fume-Modified Cement Paste," *ACI Materials Journal*, V. 93, No. 6, Nov.-Dec. 1996, pp. 539-543.
33. Macphie, D. E.; Lachowski, E. E.; and Glasser, F. P., "Polymerization Effect in C-S-H: Implications for Portland Cement Hydration," *Advances in Cement Research*, V. 1, 1988, pp. 131-137.
34. Bentz, D. P., "Effects of Cement PSD on Porosity Percolation and Chemical Shrinkage," *Self-Desiccation and Its Importance in Concrete Technology II*, B. Persson and G. Fagerlund, eds., Lund Institute of Technology, Lund, Sweden, 1999, pp. 127-134.
35. Young, J. F., "A Review of the Pore Structure of Cement Paste and Concrete and Its Influence on Permeability," *Permeability of Concrete*, SP-108, D. Whiting and A. Walitt, eds., American Concrete Institute, Farmington Hills, Mich., 1988, pp. 1-19.
36. Bentz, D. P., and Garboczi, E. J., "Simulation Studies of the Effects of Mineral Admixtures on the Cement Paste-Aggregate Interfacial Zone," *ACI Materials Journal*, V. 88, No. 5, Sept.-Oct. 1991, pp. 518-529.
37. Villadsen, J., "Hærdetemperaturens Indflydelse På Hærdnet Cementpastas Porestruktur: Projekttrapport," The Technical University of Denmark, Lyngby, Denmark, 1989.
38. Hooton, R. D., personal communication, Dec. 2004.